Suggestions for Experimental Verification of Instrumental Responses

Steve Ellingson*

October 1, 2008

Contents

*Bradley Dept. of Electrical & Computer Engineering, 302 Whittemore Hall, Virginia Polytechnic Institute & State University, Blacksburg VA 24061 USA. E-mail: `ellingson@vt.edu`

1 Summary

This memo makes some suggestions about how to go about measuring the responses of prototype LWA components, including antennas (ANT), FEE, cables, and receivers (ARX). As noted previously by others, antenna patterns can be determined using observations of strong discrete sources by a two-element interferometer; the relevant math is shown and various caveats are noted. It is shown that only the magnitude of the antenna pattern, and not the phase, can be determined using the proposed method.

2 Data Model

2.1 Plane Wave Incident on Antennas

In the following model, the Cartesian coordinate system x-y-z is positioned such that the origin is in the plane of the array, with the x and y axes lying in the plane of the array and the z axis pointing toward the zenith. The zenith angle θ is measured from the z axis.

Consider a monochromatic plane wave incident from direction in which $\hat{\mathbf{r}}$, a unit vector with tail fixed to the origin, points. Let $s^{(RF)}(t,\omega')$ be the waveform associated with this plane wave, measured at the origin, and let the frequency of this waveform be $\omega_c+\omega'$. ω_c is intended to represent the center of the observed bandpass, whereas ω' is intended to represent an offset from the center frequency that will ultimately become the baseband frequency after downconversion. Thus:

$$s^{(RF)}(t,\omega') = S(\omega')e^{j(\omega_c+\omega')t} \tag{1}$$

where $S(\omega')$ is the baseband magnitude and phase of the waveform.

Let the position of the n^{th} antenna in the array be $\mathbf{p}_n$, a vector whose tail is fixed at the origin. The waveform at this point in space is

$$s_n^{(RF)}(t,\omega') = s^{(RF)}(t-\tau_n(t),\omega') = S(\omega')e^{j(\omega_c+\omega')(t-\tau_n(t))} \tag{2}$$

where $\tau_n(t)$ is the geometrical delay associated with $\mathbf{p}_n$ and is given by:

$$\tau_n(t) = \frac{-\hat{\mathbf{r}}(t)\cdot\mathbf{p}_n}{c} \tag{3}$$

where c is the speed of light and we explicitly show the time dependence of $\hat{\mathbf{r}}$ to underscore the fact this is time-varying since the sky appears to move relative to the array. It will be convenient to express $\tau_n(t)$ in the form of a polynomial. This can be done using a Taylor series expansion around time $t=t_0$ as follows:

$$\tau_n(t) = \tau_n(t_0) + \left[\frac{d}{dt}\tau_n(t)\right]_{t_0}(t-t_0) + \frac{1}{2}\left[\frac{d^2}{dt^2}\tau_n(t)\right]_{t_0}(t-t_0)^2 + \ ... \tag{4}$$

To compute the first derivative of $\tau_n(t)$ we note that $\mathbf{p}_n$ can be expressed as

$$\mathbf{p}_n = \hat{\mathbf{x}}d_n\cos\phi_n + \hat{\mathbf{y}}d_n\sin\phi_n \tag{5}$$

where d_n is the distance of the associated antenna from the origin, and ϕ_n is the associated radial coordinate in the xy plane. Similarly,

$$\hat{\mathbf{r}}(t) = \hat{\mathbf{x}}\cos\phi(t)\sin\theta(t) + \hat{\mathbf{y}}\sin\phi(t)\cos\theta(t) + \hat{\mathbf{z}}\cos\theta(t) \tag{6}$$

Thus

$$\tau_n(t) = -\frac{d_n}{c}\sin\theta(t)\cos\left[\phi(t)-\phi_n\right] \tag{7}$$

$$\frac{d}{dt}\tau_n(t) = -\frac{d_n}{c}\left[\frac{d\theta}{dt}\cos\theta(t)\cos\left[\phi(t)-\phi_n\right] - \frac{d\phi}{dt}\sin\theta(t)\sin\left[\phi(t)-\phi_n\right]\right] \quad (8)$$

For later notation convenience, let this quantity be known as α_n, which is understood to be time-varying. Note that $d\theta/dt$ and $d\phi/dt$ are both upper-bounded by the sky's apparent rate of rotation, which is simply 2π radians per day, or 7.27×10^{-5} rad/s. Thus, we can assume the upper bound for α_n when $\phi(t) = \phi_n$ is also the upper bound regardless of $\phi(t)$; so that we need only to consider the first term to determine this bound. Assuming $d_n < 1$ km (probably sufficient for the proposed experiments as explained in a later section), we find that $\alpha_n < 2.42 \times 10^{-10}$. Comparing the first two terms of the Taylor series for the minimum expected delay of $\approx$ (4 m)/c (assuming minimum 4 m spacing between stands):

$$\frac{\alpha_n \Delta t}{\tau_n(t_0)} < \left(0.0182 \text{ s}^{-1}\right)\Delta t \quad (9)$$

where $\Delta t \equiv t - t_0$. Thus, we see that under these assumptions the second term of the Taylor series becomes important at the 1% level at $\Delta t \sim 549$ ms.

Moving on to the third term of the Taylor series:

$$\frac{d^2}{dt^2}\tau_n(t) = -\frac{d_n}{c}\left(\frac{d^2\theta}{dt^2}\cos\theta(t) - \left(\frac{d\theta}{dt}\right)^2\sin\theta(t)\right) \quad (10)$$

where we have once again limited ourselves to the case $\phi(t) = \phi_n$ with the understanding that this leads to bounds applicable independent of $\phi(t)$, as discussed above. The factor $d^2\theta/dt^2$ is largest at the celestial poles, where $d\theta/dt$ oscillates between zero and the sky apparent rate of rotation every 6 hours. Thus, the magnitude of $(d^2\theta/dt^2)\cos\theta(t)$ is loosely upper-bounded by $(7.27 \times 10^{-5}$ rad/s) / (6 h) $= 3.37 \times 10^{-9}$ rad/s^2. Similarly, the magnitude of $(d\theta/dt)^2\sin\theta(t)$ is loosely upper-bounded by $(7.27 \times 10^{-5}$ rad/s$)^2 = 5.28 \times 10^{-9}$ rad/s^2. Thus the ratio of the maximum magnitudes of the second and third terms of the Taylor series is bounded as follows:

$$\frac{(1.44 d_n \times 10^{-17} \text{ rad/s}^2)(\Delta t)^2}{\alpha_n \Delta t} < \left(5.95 \times 10^{-5} \text{ s}^{-1}\right)\Delta t \quad (11)$$

Thus, we see that under these assumptions the third term of the Taylor series becomes important at the 1% level at $\Delta t \sim 168$ s. In conclusion, we shall use the approximation

$$\tau_n(t) \approx \tau_n 0 + \alpha_n(t - t_0) \quad (12)$$

where $\tau_{n0} \equiv \tau_n(t_0)$, and we assume this is valid for Δt up to 168 s.

Substituting the approximation of Equation 12 into Equation 2, we have:

$$s_n^{(RF)}(t,\omega') = S(\omega')e^{j(\omega_c+\omega')(t-\tau_{n0}-\alpha_n(t-t_0))} \quad (13)$$

Rearranging factors:

$$s_n^{(RF)}(t,\omega') = e^{j\omega_c t}e^{-j\omega_c\alpha_n t}e^{-j\omega_c\tilde{\tau}_{n0}}S(\omega')e^{-j\omega'\tilde{\tau}_{n0}}e^{+j\omega'(1-\alpha_n)t} \quad (14)$$

where $\tilde{\tau}_{n0} \equiv \tau_{n0} - \alpha_n t_0$. This can be generalized into an expression for signal of any bandwidth simply by integrating over ω':

$$s_n^{(RF)}(t) \equiv \int_{-\infty}^{+\infty} s_n^{(RF)}(t,\omega')d\omega' \quad (15)$$

Thus:

$$s_n^{(RF)}(t) = e^{j\omega_c t}e^{-j\omega_c\alpha_n t}e^{-j\omega_c\tilde{\tau}_{n0}}\int_{-\infty}^{+\infty} S(\omega')e^{-j\omega'\tilde{\tau}_{n0}}e^{+j\omega'(1-\alpha_n)t}d\omega' \quad (16)$$

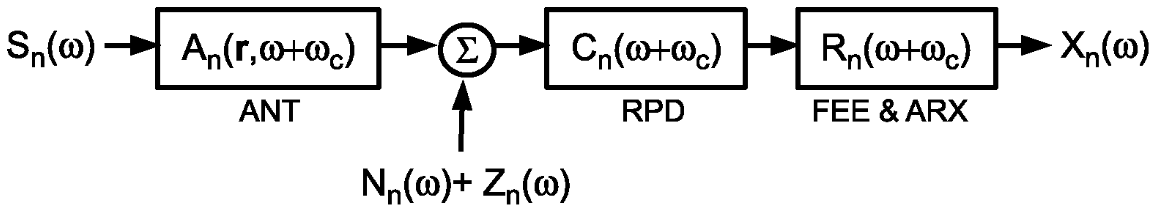

Figure 1: System Model.

The integral can be solved using the inverse Fourier transform through the change of variables $u' \equiv \omega'(1-\alpha_n)$:

$$s_n^{(RF)}(t) = e^{j\omega_c t} e^{-j\omega_c \alpha_n t} e^{-j\omega_c \tilde{\tau}_{n0}} \frac{1}{1-\alpha_n} \int_{-\infty}^{+\infty} S\left(\frac{u'}{1-\alpha_n}\right) e^{-ju'\tilde{\tau}_{n0}/(1-\alpha_n)} e^{+ju't} du' \tag{17}$$

$$s_n^{(RF)}(t) = e^{j\omega_c t} e^{-j\omega_c \alpha_n t} e^{-j\omega_c \tilde{\tau}_{n0}} \frac{2\pi}{1-\alpha_n} \mathcal{F}^{-1}\left\{ S\left(\frac{u'}{1-\alpha_n}\right) e^{-ju'\tilde{\tau}_{n0}/(1-\alpha_n)} \right\} \tag{18}$$

$$s_n^{(RF)}(t) = 2\pi e^{j\omega_c t} e^{-j\omega_c \alpha_n t} e^{-j\omega_c \tilde{\tau}_{n0}} s\left((1-\alpha_n)t - \frac{\tilde{\tau}_{n0}}{1-\alpha_n}\right) \tag{19}$$

where $s(t) \equiv \mathcal{F}^{-1}\{S(\omega)\}$; i.e., the time domain form of the full-bandwidth incident waveform. Recalling that $|\alpha_n| < 2.42 \times 10^{-10}$, the following approximation can be made with negligible error:

$$s_n^{(RF)}(t) = 2\pi e^{j\omega_c t} e^{-j\omega_c \alpha_n t} e^{-j\omega_c \tilde{\tau}_{n0}} s\left(t - \tilde{\tau}_{n0}\right) \ . \tag{20}$$

Signals will typically be downconverted to a center frequency of zero for subsequent processing, resulting in the baseband representation:

$$s_n^{(RF)}(t) e^{-j\omega_c t} = 2\pi e^{-j\omega_c \alpha_n t} e^{-j\omega_c \tilde{\tau}_{n0}} s\left(t - \tilde{\tau}_{n0}\right) \tag{21}$$

Canceling of the factor $e^{-j\omega_c \alpha_n t}$ is desirable if the phase $\omega_c \alpha_n \Delta t$ is significant, as signals obtained from different antennas will not be coherent with respect to each other otherwise. For 88 MHz and $\alpha_n = 2.42 \times 10^{-10}$, this phase changes by 1° in $\Delta t = 130$ ms. Therefore, it should be dealt with. We have:

$$s_n(t) \equiv s_n^{(RF)}(t) e^{-j\omega_c t} e^{+j\omega_c(\alpha_n t + \tilde{\tau}_{n0})}/(2\pi) = s\left(t - \tilde{\tau}_{n0}\right) \tag{22}$$

where we have chosen to simultaneously cancel the nuisance phase factor $e^{-j\omega_c \tilde{\tau}_{n0}}/(2\pi)$ since essentially no additional work is required to do this.

Before moving on, we repeat that this is an approximation because the sky is moving with respect to the array but only the lowest-order (linear) terms in the associated Taylor series expansion of $\tau_n(t)$ have been taken into account. We use $\tilde{\tau}_{n0} \equiv \tau_{n0} - \alpha_n t_0$ (as opposed to simply τ_{n0}) to account for phase error associated with the re-computation of the Taylor series expansion at each new t_0, and note that the above expression should not be assumed to be valid for more than ~ 168 s at a time; i.e., that τ_{n0} and α_n should be recomputed at least that often.

2.2 System Model

The system model is shown in Figure 1. Note that this is a frequency-domain model. Components of the model are explained below.

- $S_n(\omega) \equiv \mathcal{F}\{s_n(t)\} = S(\omega)e^{-j\omega\tilde{\tau}_{n0}}$, the incident electric field spectrum at position $\mathbf{p}_n$, having units of V m^{-1} Hz$^{-1/2}$.
- $N_n(\omega)$ represents the external (hopefully, sky) noise measured at the terminals of the antenna at position $\mathbf{p}_n$, having units of V m^{-1} Hz$^{-1/2}$. Note this noise is modified from the noise which actually appears at the antenna terminals, since it is subjected to the same downconversion and fringe stopping operations experienced by the signal of interest.
- $A_n(\hat{\mathbf{r}}, \omega+\omega_c)$ describes the antenna (ANT) response in the direction $\hat{\mathbf{r}}$, and has units of meters (i.e., effective length) such that the output has units of V Hz$^{-1/2}$.
- $Z_n(\omega+\omega_c)$ is internally generated noise, referenced to the input of the FEE and having units of V Hz$^{-1/2}$. It is assumed that this noise originated from the FEE and dominates over the noise contribution of the ARX. Note this noise is modified from the noise which is actually generated, since it is subjected to the same downconversion and fringe stopping operations experienced by the signal of interest.
- $C_n(\omega+\omega_c)$ describes the response of cables and associated hardware (RPD), and is unitless.
- $R_n(\omega+\omega_c)$ describes the combined response of the front end electronics (FEE) and receiver (ARX), and is unitless.
- $X_n(\omega)$ is the captured signal after downconversion to a center frequency of zero and fringe stopping (per Equation 22), having units of V Hz$^{-1/2}$.

Thus we have

$$X_n(\omega) = R_n(\omega+\omega_c)C_n(\omega+\omega_c)\left[A_n(\hat{\mathbf{r}}, \omega+\omega_c)S_n(\omega) + N_n(\omega) + Z_n(\omega)\right] \tag{23}$$

The explicit display of frequency dependence becomes tedious, so we shall use the equivalent "shorthand" expression:

$$X_n = R_n C_n \left[A_n(\hat{\mathbf{r}})S_n + N_n + Z_n\right] \tag{24}$$

Correlation between two signals X_n and X_m is defined as follows:

$$X_{nm} \equiv \langle X_n X_m^* \rangle \tag{25}$$

where the superscript asterisk denotes conjugation and the angle brackets denote time-averaging (i.e., integration). As noted above, integration for more than $\sim$ 168 s is not recommended. Assuming the internal and external noise is uncorrelated, and assuming that the noise from any given FEE is uncorrelated with the noise from any other FEE, we find using the model of Equation 24 that:

$$X_{nm} = R_n R_m^* C_n C_m^* \left(A_n(\hat{\mathbf{r}})A_m^*(\hat{\mathbf{r}})|S|^2 e^{-j\omega(\tilde{\tau}_{n0}-\tilde{\tau}_{m0})} + \langle N_n N_m^* \rangle \right) \tag{26}$$

3 Determination of Model Parameters

We now consider how to determine the model parameters appearing in Equation 26.

The cable and receiver responses C_n and R_n can be determined experimentally before observing. It is important that this measurement be coherent (i.e., include phase), since it is important to capture the delay and dispersion characteristics. The simplest approach is simply to use a vector network analyzer to measure s_{12}. Cable can also be measured in terms of s_{11} by short circuiting the opposite end and then accounting for the round trip (vs. one-way) propagation and the reflection coefficient of -1. An alternative to a vector network analyzer that uses the same data acquisition

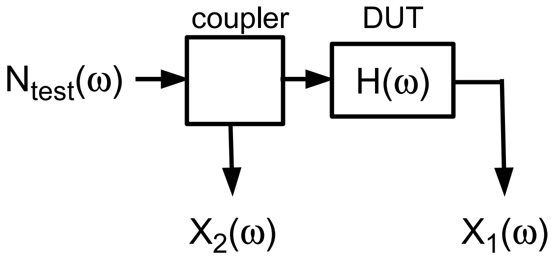

Figure 2: One possible method for determining the complete (magnitude and phase) response of a component.

used for interferometry is shown in Figure 2. In this approach, a noise source generates N_{test}, the response to be determined is H, and the acquired data are:

$$X_1 = HG_tN_{test} \tag{27}$$

$$X_2 = G_cN_{test} \tag{28}$$

where G_c and G_t are the "coupled" and "through" port responses of the coupler. Thus,

$$X_{12} = G_c^*G_tH\sigma_{test}^2 \tag{29}$$

where $\sigma_{test}^2 = \left\langle |N_{test}|^2 \right\rangle$. Thus:

$$H = \frac{X_{12}}{G_c^*G_t\sigma_{test}^2} \tag{30}$$

and $G_c^*G_t$ can be determined using the exact same expression for a separate measurement in which the device under test is replaced with a through connection; i.e., $H = 1$.

Next, consider the noise term $\langle N_nN_m^* \rangle$. Since we intend to be sky noise dominated, N_n and N_m are guaranteed to be correlated. Thus, $\langle N_nN_m^* \rangle$ does not necessarily approach zero with increasing integration. If the sky noise temperature were constant with respect to $\hat{\mathbf{r}}$, this would result in $\langle N_nN_m^* \rangle$ having a large constant value, and thus would be a simple bias that could be easily removed. However, the presence and sidereal motion of other sources – the Galactic plane in particular – causes the associated bias to be time-varying as well as potentially large. Unfortunately, this correlation bias may not be sufficiently suppressed by fringe stopping for the desired source (e.g., Cas A). However, the degree of suppression offered by fringe stopping for distributed sources can be increased by increasing the separation between the antennas until the associated waveform at the two antennas becomes decorrelated. This is equivalent to spatially resolving the nuisance feature. Since the spatial resolution of a two-element interferometer is λ/D, a feature having angular extent ψ is resolved for a baseline $D > \lambda/\psi$. To resolve sources down to 10° with factor-of-10 overkill requires $D = 1.72$ km at 10 MHz, 452 m at 38 MHz, 232 m at 74 MHz, and 195 m at 88 MHz. If this condition is satisfied, it is probably safe to assume $\langle N_nN_m^* \rangle$ is negligible; however it would be prudent to evaluate this both through sky-model simulation and experimentally.

Finally, consider the incident power density factor $|S|^2$ in Equation 26. This has units of $\mathrm{V}^2\ \mathrm{m}^{-2}\ \mathrm{Hz}^{-1}$. By plane wave theory, we can relate this to the flux P of the source being observed (e.g., Cas A), which has units of $\mathrm{W\ m}^{-2}\ \mathrm{Hz}^{-1}$, through the plane wave relationship $P = |S|^2/(2\eta)$ where $\eta \approx 377\ \Omega$ is the wave impedance in free space. Thus, $|S|^2 = 2\eta P$.

We can now calculate the following quantity related to the antenna response:

$$A_n(\hat{\mathbf{r}})A_m^*(\hat{\mathbf{r}}) = \frac{X_{nm}}{R_nR_m^*C_nC_m^*|S|^2e^{-j\omega(\tilde{\tau}_{n0}-\tilde{\tau}_{m0})}} - \frac{\langle N_nN_m^* \rangle}{|S|^2e^{-j\omega(\tilde{\tau}_{n0}-\tilde{\tau}_{m0})}} \tag{31}$$

If the antennas are identical and oriented in exactly the same way, we find:

$$A_n(\hat{\mathbf{r}})A_m^*(\hat{\mathbf{r}}) = |A_n(\hat{\mathbf{r}})|^2 \tag{32}$$

In other words, the best we can do is to find the magnitude of the pattern; the phase of the pattern is not available. The units of $|A_n(\hat{\mathbf{r}})|$ are m^2; however this is *effective length* squared, which is not the same as the effective (collecting) area, A_e. Furthermore, it is often desired to express antenna pattern magnitude in dBi. To accomplish this, we note that the power delivered by the antenna is

$$P_A = \frac{|\mathbf{E}^i|^2}{2\eta} A_e(\hat{\mathbf{r}}) \tag{33}$$

where $\mathbf{E}^i$ is the electric field spectral density vector. This can also be determined in terms of the impedance of the antenna impedances $Z_A = R_A + jX_A$ and load impedance R_L as:

$$P_A = \frac{1}{2} \frac{|\mathbf{E}^i \cdot \mathbf{l}_e(\hat{\mathbf{r}})|^2 R_L}{|Z_A + R_L|^2} \tag{34}$$

where $\mathbf{l}_e(\hat{\mathbf{r}})$ is the vector effective length of the antenna. (This expression is easily derived using the Thevenin equivalent circuit model of a receive antenna with R_L connected at the terminals.) Equating the two expressions above we find:

$$A_e(\hat{\mathbf{r}}) = \eta \frac{|\hat{\mathbf{e}}^i \cdot \mathbf{l}_e(\hat{\mathbf{r}})|^2 R_L}{|Z_A + R_L|^2} \tag{35}$$

where $\hat{\mathbf{e}}^i$ is the unit-magnitude vector describing the polarization of $\mathbf{E}^i$. Separately (also from the Thevenin equivalent circuit model), note that:

$$|A_n(\hat{\mathbf{r}})|^2 = \frac{1}{4} |\hat{\mathbf{e}}^i \cdot \mathbf{l}_e(\hat{\mathbf{r}})|^2 \left(1 - |\Gamma|^2\right) \tag{36}$$

where

$$\Gamma \equiv \frac{Z_A - R_L}{Z_A + R_L} \tag{37}$$

Thus:

$$|A_n(\hat{\mathbf{r}})|^2 = |\hat{\mathbf{e}}^i \cdot \mathbf{l}_e(\hat{\mathbf{r}})|^2 \frac{R_L^2}{|Z_A + R_L|^2} \tag{38}$$

substituting into Equation 35, we have:

$$A_e(\hat{\mathbf{r}}) = \frac{\eta}{R_L} |A_n(\hat{\mathbf{r}})|^2 \tag{39}$$

Since the gain G (over isotropic) of an antenna is $4\pi A_e/\lambda^2$, we find:

$$G(\hat{\mathbf{r}}) = \frac{4\pi\eta}{R_L \lambda^2} |A_n(\hat{\mathbf{r}})|^2 \tag{40}$$

4 Suggested Test Procedure

The following sequence of tasks is suggested:

1. Measure R_n for all FEE+ARX combinations to be employed. Compare to predicted values.
2. Measure C_n for all cables to be employed. Compare to predicted values. In particular, compare observed and predicted dispersion.
3. If possible, determine $R_n C_n$ for all n after field deployment, to confirm that it has not changed since the above measurements.

4. Determine N_n for each antenna/channel separately, using Equation 24 with a model for the frequency response of the antenna (e.g., using NEC2). Compare to established values for N_n. Both the frequency response and diurnal variation are of interest. In this way, antenna models can be validated, which is useful for the next step.

5. It would be useful to perform an stability test at this point to determine the length of time over which all channels are gain- and phase-stable. This may be somewhat difficult to do *in situ* considering sky-noise-dominated antennas are involved, because the spatial distribution of noise on the sky is constantly changing. Upon installation, it could be useful to do the following test: Disconnect cables from FEEs and connect them together to the output ports of single splitter, which is fed by a noise source. (If suitable differential "plumbing" can be constructed, FEEs can be included in this test.) Instead of correlation, compute $< X_n/X_m >$ pairwise among the cables; this gives magnitudes that are nominally unity and phases that are nominally zero. This test can also be repeated using antennas with the sky as the stimulus, however in that case only the magnitudes are expected to be nominally constant.

6. Using Equation 26 without tracking, and preferably when any bright discrete sources are at low elevation or below the horizon, determine $\langle N_n N_m^* \rangle$. The idea is to do this at times when the contribution from any potential "$|S|^2$" (Cas A, Cyg A, etc) is negligible. This should probably be done for a few times during the day. Compare to simulation if possible. Compare $\langle N_n N_m^* \rangle$ to $|S|^2$ for proposed source(s) to determine if $\langle N_n N_m^* \rangle$ is negligible, or if it must be dealt with explicitly (by including it in the calculation) or by suppressing it (by increasing the separation between antennas).

7. Determine $G(\hat{\mathbf{r}})$ for a track through the sky using Cas A with Equations 31 and 40. This is of course a function of frequency; however the priority is higher frequencies where concerns about the antenna pattern are greatest. Both of the raw polarizations of the antenna are of interest.

5 Document History

- Version 2 (October 1, 2008): Cleaned up various mathematical details and revised the model, which was not quite correct in the previous version. No conclusions are affected.
- Version 1 (July 2, 2008): First version.